Macromolecules

ARTICLE

pubs.acs.org/Macromolecules

Salt Species-Dependent Electrostatic Effects on ssDNA Elasticity

D. B. McIntosh[†] and O. A. Saleh[*,‡]

[†]Physics Department, University of California, Santa Barbara, California 93106, United States

[‡]Materials Department and BMSE Program, University of California, Santa Barbara, California 93106, United States

ABSTRACT: The interactions of charged, flexible polymers with counterions of various valencies is a fundamental unsolved problem of polyelectrolyte physics, with specific applications to structure formation by nucleic acids, including RNA folding and DNA nanotechnology. We recently showed that single-molecule measurements of the elasticity of a model polyelectrolyte, denatured single-stranded DNA (d-ssDNA), can reveal details of the polymer's electrostatic interactions on multiple length scales. Here, we explore the effects of various salts on d-ssDNA elasticity. In agreement with our prior results in NaCl, we find that d-ssDNA elastic response in KCl, $MgCl_2$, and $CaCl_2$ shows a low-force Pincus regime, with a weaker response at higher forces. The data in KCl are quantitatively identical to prior NaCl data, reflecting the universality of monovalent salt electrostatics. In contrast, the behavior of d-ssDNA in divalent salt solutions shows subtantial quantitative differences, including a nonlogarithmic high-force behavior and a heightened sensitivity of elasticity to changes in divalent salt concentration. We introduce a condensed-ion model that can quantitatively account for some aspects of this sensitivity.

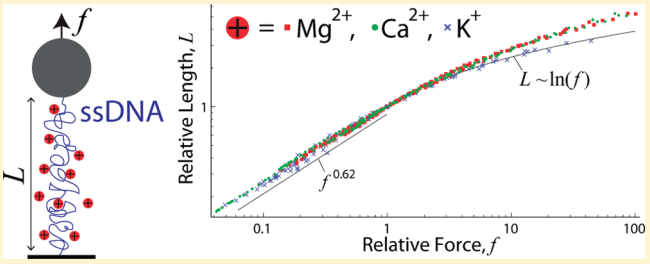

INTRODUCTION

Electrostatic forces play a dominant role in determining the structure and function of charged macromolecules in solution. DNA, RNA, and many proteins are highly charged and must overcome a large electrostatic energy in order to fold into their native states. To do this, these macromolecules interact with oppositely charged salt ions in solution to screen intramolecular interactions. Understanding the physics of these interactions would be a major step forward for both our understanding of basic processes in molecular biology (e.g., collapse and stabilization of proteins and ion-mediated RNA folding) and our ability to exploit macromolecules for technological purposes (e.g., design of self-assembling nanostructures, macromolecular drugs, and aptamers).

The electrostatics of monovalent salts are relatively well-understood up to moderate concentrations using mean-field theories: the Poisson−Boltzmann approach, and even the Debye−Huckel approximation, agree well with computer simulations and experiments.[1] In contrast, the behavior of multivalent ions is relatively poorly understood, as strong ion−ion interactions disallow the mean-field approach. Simultaneously, multivalent ions induce dramatic and multifaceted phenomena in macromolecules: they are capable of fully neutralizing, and even reversing, the charge of macroions,[2] and of collapsing charged polymers.[3] They also play a pivotal role in the formation of secondary structure in RNA and proteins[4] and the stabilization of DNA nanostructures which can self-assemble despite significant internal structural stress.[5,6]

In prior work, we showed that a new experimental approach, single-molecule elasticity at low forces (SM-ELF), is a sensitive probe of the structural parameters of a charged polyelectrolyte.[7,8] SM-ELF uses magnetic tweezers to measure the extension of single polymer molecules at a variety of forces. The force has the effect of screening out long-range monomer interactions. Varying the force probes various length scales in the polymer: the higher the force, the shorter the length scale probed. Thus, analysis of the resulting force−extension curves in the context of robust scaling models permits the estimation of important physical parameters such as the Kuhn length and excluded volume which are difficult to measure by other means.[8]

We previously applied SM-ELF to the study of permanently denatured single-stranded DNA ("d-ssDNA") in a variety of NaCl concentrations.[7,8] This work revealed a regime of real-polymer elasticity, the "Pincus blob" regime, and permitted the quantification of the dependence of the polymer's Kuhn length, l, and excluded volume parameter, ν, on added monovalent salt (NaCl). Further, SM-ELF data on d-ssDNA permitted precise measurement of both the onset of salting-out (i.e., the salt-induced Θ point) and the intrinsic (nonelectrostatic) persistence length of the polymer.

Here, we utilize the SM-ELF approach to study ion-specific and multivalent-ion effects on polyelectrolyte behavior. In particular, we measure the elasticity of d-ssDNA in solutions containing varying concentrations of KCl, $MgCl_2$, or $CaCl_2$. We find that the Pincus regime is accessible at low forces for all salts studied here but that the transition out of this regime is different in multivalent and monovalent salts. In KCl, the elasticity is nearly identical to that found previously for NaCl:[7,8] universal elastic

Received: December 14, 2010
Revised: February 9, 2011
Published: March 11, 2011

behavior is found by rescaling the force-extension curves by a salt-dependent force f_c, which demarcates the low-force Pincus regime and a high-force logarithmic regime. The salt dependence of the crossover, $f_c \sim [\mathrm{KCl}]^{0.47\pm0.03}$, indicates the Kuhn length varies as $l \sim 1/[\mathrm{KCl}]^{1/2}$, consistent with results in NaCl[7,8] and inconsistent with the well-known Odijk−Skolnick−Fixman (OSF) theory.[9,10] In both 2:1 salts, the high-force logarithmic behavior is not seen, but we still find universal behavior upon rescaling by a force $\bar{f}$. However, the rescaling parameter is much more sensitive to salt when divalents are present: we find $\bar{f} \sim I^3$, where I is the ionic strength of the solution (divalent + buffer). Further indicating sensitivity to divalents, we find that equivalent elastic behavior is found between 2:1 salts and 1:1 salts when the former are 50−200 times less concentrated; this ratio persists in both the good- and Θ-solvent regimes. In the high-salt limit, we account for this equivalency ratio by modeling the valency-dependent condensation of hydrated ions onto the charged polymer.

METHODS

We create denatured ssDNA (d-ssDNA) tethers by enzymatic methods as previously discussed.[8] Briefly, we synthesize a 10.5 kbp segment of double-stranded DNA from the lambda genome using Expand Long-Template PCR kit (Roche) and two 5′-biotinylated primer oligomers (IDT). The product is then gel purified before modifying the 3′ ends with digoxigenin-dUTP (Roche) using terminal transferase (NEB). After a final purification with PCR quick cleanup kit (Invitrogen), the double-stranded construct is thermally denatured at 90 °C in the presence of DMSO (Fisher) for 10 min followed by permanent denaturation with 1 M glyoxal (Fluka) for 1 h at 50 °C.[11] Glyoxal is an aldehyde that covalently binds to the hydrogen-bonding amine sites on the ssDNA bases, thus preventing intrastrand base-pairing. The use of glyoxal is a common strategy for minimizing secondary structure in nucleic acids.[11,12] While ssDNA cross-linking has been observed in the presence of glyoxal, it is a function of reaction conditions.[13] We minimize cross-linking by reacting with extreme excess of glyoxal at high temperature.

These tethers are attached at one end to an antidigoxigenin-coated coverslip and the other to a streptavidin-coated paramagnetic bead. The tether is then manipulated using standard magnetic tweezers protocols[14] to produce the force−extension curves presented here. All data presented are taken from high force to low force. In some cases, hysteresis was tested and the effects were negligible for the conclusions presented. Specifically, particularly at high salt, some molecules are shorter upon return to high force. However, upon scaling by the extension at 10 pN, the data collapse as presented. Previous experiments[7,8] were performed in 5 mM phosphate buffer at pH 6.5, which is incompatible with solutions containing calcium ions. Data in divalent salts are in a background of 10 mM Trizma hydrochloride buffer (Sigma) at pH 7.5, with the desired concentration of chlorine salt added from concentrated stock solutions. Both 10 mM tris, pH 7.5, and 5 mM phosphate buffer, pH 6.5, have an ionic strength and monovalent cation concentration of ≈8 mM. In the absence of added salt, force−extension behavior of d-ssDNA in the two buffers is identical within the measured experimental error (data not shown).

All force−extension curves presented here are scaled by the extension at 10 pN. We choose to present the data in this way, as opposed to the conventional presentation of L/L_0, where L_0 is the contour length, because L_0 is particularly difficult to extract for d-ssDNA. The contour length varies from molecule to molecule even given identical solution conditions, presumably due to nonspecific adsorption to the surface, precluding estimation of L_0 from knowledge of the substrate design. In addition, as will be discussed, the data are not adequately described by models that asymptote to the contour length at high force. However, given estimates of the Kuhn length of ssDNA in NaCl solutions from our prior study[7] (≈1.2−5 nm as you change from 3 M to 20 mM), the wormlike chain model[15,16] predicts that the extension at 10 pN varies between approximately 60% and 80% of the full contour length.

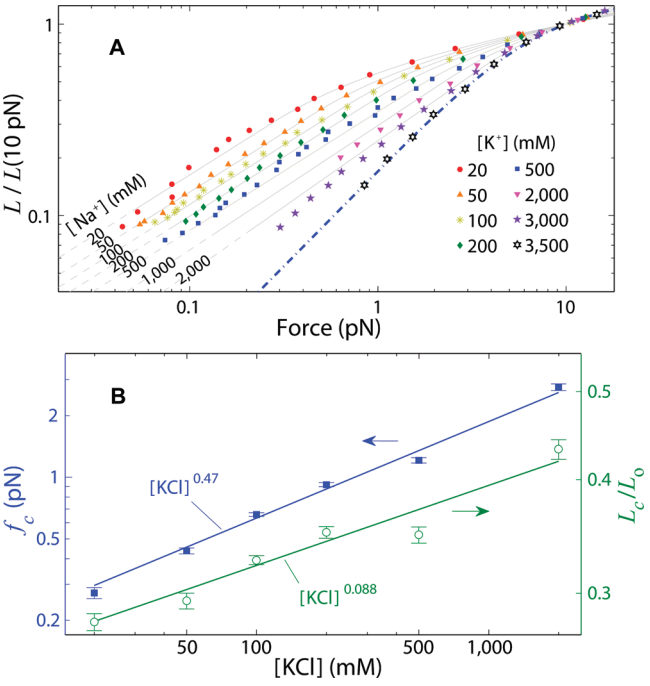

Figure 1. (A) Force−extension data on d-ssDNA from 20 mM to 3.5 M KCl. Gray curves in the background represent consensus behavior in NaCl at the specified concentration as documented previously.[7] The blue dash-dotted line is a WLC with persistence length 0.62 nm. (B) Crossover force f_c and relative crossover length L_c/L_0 versus the concentration of KCl; solid lines indicate best-fit power laws.

MONOVALENT SALT: ION-SPECIFIC EFFECTS

Here, we exchange the NaCl in the previous study[7] with KCl to investigate chemistry-dependent effects of monovalent salts. Force−extension data on d-ssDNA in various KCl solutions are plotted in Figure 1A. The background curves show the consensus d-ssDNA force−extension behavior over a range of NaCl concentrations (20 mM to 2 M).[7] The agreement between the force−extension behavior between the two salts, at least up to moderate concentrations, reflects the universality of monovalent salt electrostatics.

Force−extension behavior in 20 mM < [KCl] < 2 M fits well to the model described previously.[7] At low force, the polymer is in the "Pincus regime": it is well-described as a chain of tensile blobs of size $\xi = k_BT/f$. Within these tensile blobs excluded volume interactions are significant and swell the polymer, but monomers separated by more than ξ are well-separated by the force. Application of this scaling model yields the power-law prediction $L \sim f^{2/3}$.[17] As the force increases, the tensile screening length decreases until long-range interactions within the tensile blobs become insignificant. Prior considerations indicate that, for d-ssDNA, this occurs at a crossover force $f_c \sim k_BT/l$ and a crossover extension $L_c/L_0 \sim (\nu/l^3)^{1/3}$.[8] Beyond this force the extension varies logarithmically with force, $L \sim \ln(f)$, as seen in prior studies of ssDNA at both moderate and high forces.[12,18] The logarithmic regime is not well-understood from a theoretical

standpoint. However, it does persist for more than a decade in force at low monovalent salt concentrations. It is possible that the logarithm arises as a smooth transition between the "Pincus regime" and known ideal polymer behavior such as the wormlike chain[16] or a recently proposed discrete chain model for flexible polymers.[19]

We analyze the data to extract estimates of the salt dependence of l and ν: We estimate the power law exponent by fitting only the low-force data. Then, we fix the exponent at each salt concentration and fit the entire curve with a function that transitions smoothly and continuously from the power-law to logarithmic regime.[7] This fit returns estimates of the two parameters, f_c and L_c; the value of L_0 is estimated as the extension extrapolated from the model at 20 pN. Figure 1 shows the crossover parameters f_c and L_c/L_0 plotted as a function of KCl concentration. The data are linear on the log−log plots indicating power-law dependencies. This data allows us to estimate the salt dependence of l and ν, yielding $l \sim [\mathrm{KCl}]^{-0.47\pm0.03}$ and $\nu \sim [\mathrm{KCl}]^{-1.13\pm0.14}$, in good agreement with NaCl data ($l \sim [\mathrm{NaCl}]^{-0.51\pm0.04}$ and $\nu \sim [\mathrm{NaCl}]^{-1.09\pm0.17}$).[7] Thus, the KCl data confirm and strengthen our prior result that flexible polyelectrolytes exhibit a linear increase of Kuhn length with Debye length, in contradiction with the OSF theory.

Above ≈500 mM the NaCl and the KCl data begin to diverge. These differences appear significant in Figure 1A and may in fact be due to subtle differences in interaction between ssDNA and the different ion chemistries. However, caution is needed in interpreting the data, as the tether-to-tether variation in the high salt regime is quite large, decreasing the statistical significance of the observed difference. That said, a similarly small difference between Na ions and K ions has been measured before in the context of folding of a ribozyme,[20] though at concentrations an order of magnitude lower.

Finally, at ∼3.5 M KCl, the low-force nonlinear elasticity associated with real polymer behavior disappears and is replaced by a linear curve. Linear elasticity is characteristic of an ideal polymer, so we interpret this salt concentration as a Θ point of the polymer and exploit it to fit the wormlike chain (WLC) model of ideal polymer elasticity.[15,16] Use of the WLC model is supported by our prior results, in which WLC fits outperformed freely jointed chain fits at the Θ points in NaCl, and by several theoretical works that predict WLC behavior is expected in the moderate force range that we access.[19,21,22] As shown in Table 1, the fitted persistence length in KCl is nearly identical to that found in NaCl: $l_p \approx 0.65$ nm.

DIVALENT SALT EFFECTS

Phenomenology. In Figure 2 we show force−extension data on d-ssDNA in various concentrations of $MgCl_2$ and $CaCl_2$ in 10 mM Tris buffer at pH 7.5. For low and moderate divalent salt concentrations (0.2−10 mM), individual force−extension curves have a shape roughly similar to those in the good-solvent regime in monovalent salt: at low force, the curves exhibit a power law with exponent near 2/3, indicative of the elasticity of a swollen polymer. As the force increases, this Pincus-regime behavior is replaced with a weaker increase of length with force. Whereas the monovalent data followed a logarithmic dependence in the high force regime, the divalent data do not clearly show a logarithmic dependence in the force range that we access (see inset to Figure 3A and the discussion below).

Table 1. Persistence Length of d-ssDNA from WLC fits in Θ Conditions

salt	concentration (mM)	l_p (nm)
NaCl	3000	0.69 ± 0.03
NaCl	3500	0.60 ± 0.02
KCl	3500	0.66 ± 0.02
$MgCl_2$	50	0.64 ± 0.03
$CaCl_2$	20	0.61 ± 0.02

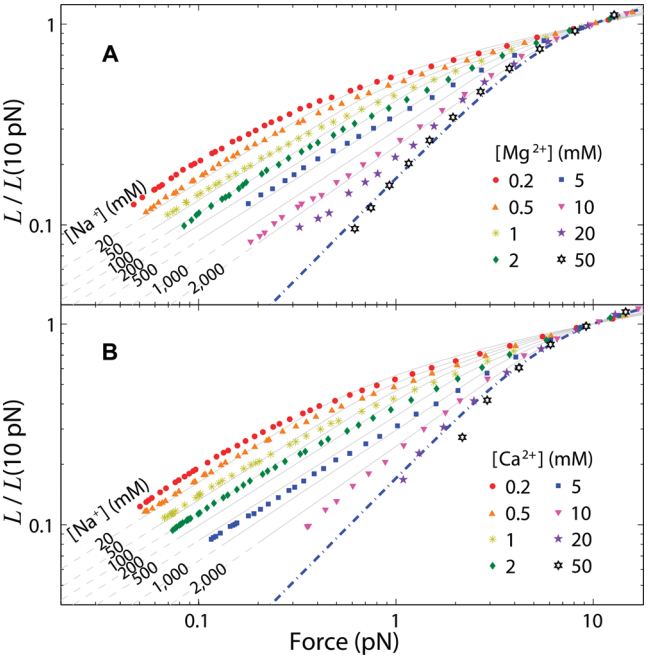

Figure 2. Force−extension behavior of d-ssDNA in 2:1 salt solutions of (A) $MgCl_2$ and (B) $CaCl_2$. For comparison, we plot gray curves in the background that represent consensus behavior in NaCl at various concentrations; the blue dash-dotted line is a WLC with persistence length 0.62 nm.

Varying divalent salts affects d-ssDNA elasticity in a qualitatively similar way to varying monovalent salt: at a given force, increasing the concentration of divalent salt causes a decrease in tether extension. For moderate increases in salt, the low-force Pincus regime is still observed, but at higher concentration the low-force elasticity becomes linear, indicating a Θ condition. Estimated persistence lengths at the Θ point, extracted from WLC-model fits,[15,16] are shown in Table 1 and indicate that l_p is nearly identical in monovalent and divalent Θ conditions.

Closer comparison of the monovalent and divalent data reveal significant quantitative differences: in the Pincus regime, a given concentration of divalent salt causes similar force-extension behavior to that found in 50- to 200- fold larger concentrations of monovalent salt (Figure 2); e.g., 1 mM $MgCl_2$ gives an elastic response roughly equivalent to 50 mM NaCl, and so on. Similar relationships are followed at the Θ points: the Pincus regime is replaced by linear behavior at ≈20 mM $CaCl_2$ and at ≈50 mM $MgCl_2$, which is respectively 150- and 60-fold less concentrated than the monovalent Θ point.

Condensed-Ion Model Accounts for Divalent Efficiency. That divalent salts are roughly 100 times more efficient than monovalent salts in affecting d-ssDNA elasticity cannot be

explained by the Debye−Huckel picture of a diffuse cloud of screening counterions. This approach generally considers electrostatic effects to be a function of the ionic strength, $I = 1/2\Sigma_i q_i^2 c_i$, where the sum is over all ions species in the solution, q_i is their valence, and c_i their concentration. Constant ionic strength results by replacing a 1:1 salt with a 2:1 salt at a 3-fold lower concentration; clearly, our results indicate a larger ratio.

A better explanation for the measured effects of divalents can be found by considering the balance between ions condensed on the charged polymer, with chemical potential μ_C, and those free in solution, with chemical potential μ_S. Our model is motivated by work on electrostatic effects in RNA folding,[20] along with strongly correlated liquid (SCL) models of counterion/macroion interactions.[23] The use of the latter model is supported by predictions of the conditions that cause polymer neutrality: for microscopic parameters appropriate for double-stranded DNA, the SCL model predicts neutralization occurs at roughly 30 mM for divalent ions.[23] This is in good agreement with our measured Θ points in divalent ions. Indeed, direct transfer of the double-stranded DNA SCL result to d-ssDNA is justified by their similar surface charge densities, a key parameter in the SCL model: compared to double-stranded DNA, single-stranded DNA has roughly half the bare linear charge density and half the radius, thus the same effective surface charge density.

We assume the polymer is closely associated with a number of condensed ions. Repulsions between the condensed ions keep them separated at a characteristic distance D. The chemical potential of the condensed ions is dominated by the electrostatic attraction of the ion to its "patch" of charged polymer: given a polymer charge density e/b, and a counterion valency z, this gives

$$\mu_C/k_BT \approx -\frac{zDl_B}{br} \qquad (1)$$

where k_BT is the thermal energy, l_B is the Bjerrum length, and r is the characteristic distance between the counterion and the charges on the polymer. Equation 1 assumes a point-charge potential for the charged polymer, rather than the logarithmic potential usually taken for cylindrical geometries. We justify that choice on two grounds: First, we consider very large concentrations of counterions and thus very short screening lengths—so, condensed counterions only interact locally with a small section of the polymer and not a long line of charges. Second, the intrinsic flexibility of d-ssDNA could allow it to slightly wrap around the counterion, bringing multiple polymer charges to roughly similar distances from the counterion, rather than dispersing the charges in a rigid linear array.

In equilibrium, $\mu_C = \mu_S$. We estimate μ_S from the volume fraction, ϕ, of ions in the bulk: $\mu_S = k_BT \ln(\phi)$. The volume fraction is $\phi = N_{Av}wc$, where N_{Av} is Avogadro's number, w is the volume per ion, and c is the molar concentration. By balancing the chemical potentials, we solve for $\nu = zb/D$, the fraction of bare charges on the polymer that are neutralized by the condensed ions:

$$\nu = -\frac{z^2 l_B}{r \ln(\phi)} \qquad (2)$$

We then posit that two different solutions, with respective parameters z_1, ϕ_1, r_1 and z_2, ϕ_2, r_2, will cause the polymer to behave identically if the charge densities (after condensation) are equivalent, i.e., if $\nu_1 = \nu_2$. Since the ions we consider here have roughly equal sizes and hydration radii, we take $r_1 = r_2$, giving the following simplified equivalency condition:

$$\phi_1^{z_2^2} = \phi_2^{z_1^2} \qquad (3)$$

In particular, for mono- vs divalent counterions, this gives $\phi_1^4 = \phi_2$, where the subscript indicates the counterion valency. We then predict the ratio of equivalent concentrations to be $c_1/c_2 = 1/\phi_1^3$, where we again assume the ions have roughly equal sizes, $w_2 = w_1$.

We expect the condition of equal charge density to be most apt for Θ conditions, since Θ likely corresponds to near-complete neutralization of the polymer. So, for monovalents, we have $c_1 \approx 3$ M. We estimate w_1 from the size of a hydrated ion: small cations typically are hydrated by 5−6 water molecules, giving a size $w_1 \approx 150$ Å^3. This predicts the equivalency ratio $c_1/c_2 \approx 50$, which is in good agreement with the measured ratio of Θ concentrations.

As c_1 decreases from Θ, the polymer enters the good solvent regime, and the measured equivalency ratio appears to increase. This is particularly evident in the Mg data, where $c_1 = 2$ M is matched by $c_{Mg} \approx 10$ mM, a ratio of 200, compared to the Θ-point ratio of 60. An increase follows from our model, as it predicts the ratio will increase with decreasing salt; particularly, with $c_1 = 2$ M, the model predicts a ratio of 170, in good agreement with the measured ratio of 200. However, in both Ca and Mg data, the measured ratio fails to follow the prediction as c_1 decreases further: the model predicts a strong monotonic increase with decreasing c_1, wherease the data show the ratio to stabilize and even to decrease (e.g., back to ≈50 at $c_{Mg} = 1$ mM). Failure of our model at lower salt is expected, as the assumptions underlying the condensed-ion/polymer electrostatic potential (eq 1) are no longer valid, and ion-competition effects beween divalents and monovalent buffer become significant.

Ion-Specific Effects. Our data indicate the Θ concentration of calcium, $c_{\Theta,Ca} \approx 20$ mM, is roughly 2-fold smaller than that of magnesium, $c_{\Theta,Mg} \approx 50$ mM. Our model can be extended to account for this difference using the different sizes of the two ions: while the bare Mg ion is smaller than Ca, it is more strongly hydrated, so $w_{Mg} > w_{Ca}$. Accounting for size differences also requires permitting $r_{Mg} \neq r_{Ca}$. It is possible that the electrostatic forces on condensed ions strip their hydration shells; if dehydrated, the bare ion size indicates $r_{Mg} < r_{Ca}$. Alternatively, condensed ions could remain hydrated, giving $r_{Mg} > r_{Ca}$. This question is resolved through application of the equal charge-density condition: satisfying both $\nu_{Ca} = \nu_{Mg}$ and the measured relation $c_{\Theta,Ca} < c_{\Theta,Mg}$ can only occur if $r_{Mg} < r_{Ca}$. Thus, our model qualitatively indicates the Θ-point differences between Ca and Mg are consistent with (1) known differences in the size of the two hydrated ions and (2) a stable hydration shell around condensed ions.

Relation to Other Studies. Results consistent with our data and model were found by Heilman-Miller et al. in an RNA folding study:[20] To effect the folding of a ribozyme, Na^+ or K^+ was required at roughly 100-fold higher concentration than Ba^{2+}, similar to the ratio we measure between divalent and monovalent ions. Also in that study, Mg^{2+} ions caused folding at about a 10-fold smaller concentration than Ba^{2+}. The authors attribute this result to the specific chelation of Mg by the ribozyme, whereas the Ba only associates nonspecifically. The literature consensus is that the mono- and divalent ions studied here tend to remain hydrated, interacting with nucleic acids via the phosphates in a diffuse, nonspecific manner consistent with our analysis.[4] Notable exceptions to this general trend include ion chelation in strong electrostatic potentials as in the secondary structures of some RNAs[4] and in the minor groove of dsDNA.[24] Again, this is

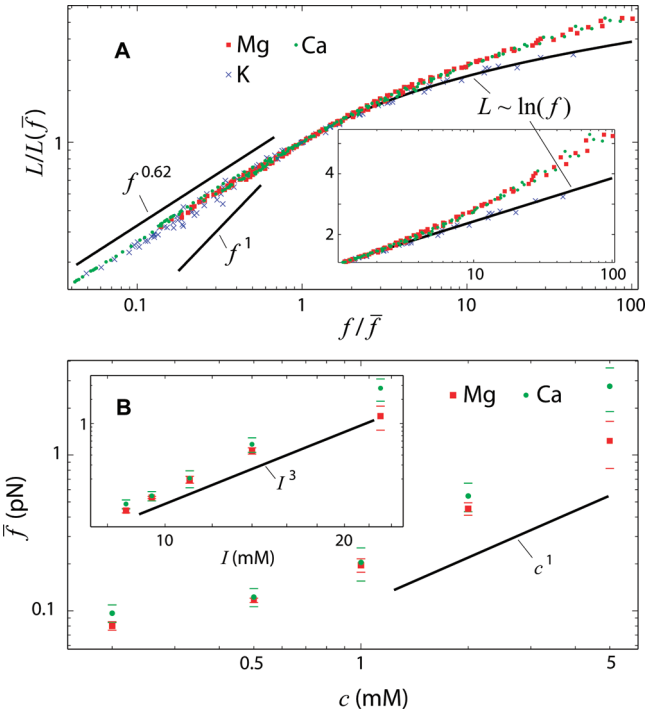

Figure 3. (A) Valence-specific collapse of force−extension curves. KCl force−extension curves collapse to a nonlinear power law at low force and a logarithm at high force when rescaled by f_c, as found for NaCl. Mg and Ca force−extension curves from 0.2 to 5 mM, when scaled by a salt-dependent $\bar{f}$ and the corresponding $L(\bar{f})$, collapse to a universal curve that differs from that of the monovalents; notably, the divalents exhibit a significantly different high-force elasticity. (B) $\bar{f}$ dependence on salt. In contrast to monovalent salts where $f_c \sim c_1^{1/2}$, we find that $\bar{f}$ does not depend as a simple power law in c_2 but appears to vary approximately as $\bar{f} \sim I^3$, where I is the ionic strength including the 8 mM monovalent buffer (inset).

consistent with our work: the chemical denaturant precludes the possibility of secondary structure in d-ssDNA, so there can be no specific ion chelation—thus, all ions in our system (including Mg) interact in a nonspecific hydrated fashion, and our hydrated, condensed ion model adequately describes the data.

More recently, Qiu et al. used small-angle X-ray scattering to probe the interactions of short double-stranded DNAs in NaCl and $MgCl_2$ solutions.[25,26] In analogy to our measurements of equivalent elastic behavior in different solutions, Qiu identified different salt conditions which gave similar inter-DNA interactions, noting particularly that 150 mM Na^+ was equivalent to 3 mM Mg^{2+}.[26] We observe a quantitatively similar effect in Figure 2. Further, they observe a weak attractive interaction between helices in the presence of ≥16 mM $MgCl_2$, the same order of magnitude as our divalent Θ concentrations, while only repulsive interactions are measured for monovalent salts up to 600 mM.[26] A similar attractive interaction may assist the collapse of d-ssDNA tethers in the present study. However, the considerations described above indicate that neutralization alone can account for much of the concentration dependence, so the attractive effect is likely a weak contribution. Finally, Qiu demonstrated that the inter-dsDNA attractive interaction slightly decreased with increasing monovalent buffer concentration, indicating the importance of ion competition.[26] Our data show a similar effect: decreasing the tris buffer concentration from 10 to 1 mM in the presence of 20 mM $CaCl_2$ causes d-ssDNA tethers to weakly aggregate as in poor solvent (data not shown).

Universal Elasticity in Good Solvent with Divalents. In monovalent salt, we were able to extract d-ssDNA's microscopic structural parameters by fitting force-extension curves with a function that described both the low-force power law and high-force logarithm. This procedure does not work with the divalent-salt curves, as the logarithmic regime does not appear, and the transition out of the power-law regime is not clean. Instead, we focus on the universal behavior of the curves: as with the monovalent data, we find that the divalent data can be rescaled by a salt-dependent factor to fall onto a common curve. We implement this by the following procedure: at each divalent salt concentration, we generate a consensus curve by aggregating data from individual tethers; for both $CaCl_2$ and $MgCl_2$ this results in five consensus curves at concentrations of 0.2, 0.5, 1, 2, and 5 mM. We choose a master curve from these five, estimate the force, $\bar{f}$, at which the power-law regime ends, and rescale the master by mapping each measured point (L,f) to a new point $(L/L(\bar{f}),f/\bar{f})$. We then perform a least-squares optimization procedure, with one free parameter, $\bar{f}$, to rescale each of the five other curves onto the master. As shown in Figure 3A, this procedure successfully collapses the 10 divalent consensus curves (five each from Mg and Ca) onto one universal plot. This procedure was robust against the choice of master: similar collapse is achieved using any of the five as the master curve (in Figure 3B we report the error in $\bar{f}$ as the standard deviation across the five different choices of master).

The ability to collapse curves across a range of salt onto a single universal curve indicates that the polymer elasticity in divalent salt is identical but for a renormalization of a fundamental microscopic length scale. In monovalent salt, we argued that this length scale is the Kuhn length and thus that the dependence of the rescaling parameter, $\bar{f} = f_c$, on ionic strength, I, can be used to report on the ionic strength dependence of the polymer's local stiffness: $l \approx k_BT/f_c \sim 1/I^{1/2}$. In divalent salt, our rescaling procedure indicates a very different dependence (Figure 3B): $\bar{f}$ does not increase simply as a power-law with divalent concentration c_2. Instead, we observe that $\bar{f}$ increases weakly with c_2 at low salt and then more strongly for $c_2 > 1$ mM. This behavior is consistent with a non-negligible electrostatic contribution of the buffer at low c_2 (as discussed above), with increasing divalent dominance at higher c_2. We attempt to account for the buffer by plotting $\bar{f}$ against total ionic strength I (inset, Figure 3B); here, the data show a strong power law, $\bar{f} \approx I^3$. Facile transfer of the previous argument would lead to the interpretation that, in divalent salt, the polymer's Kuhn length decreases as $l \sim 1/I^3$. However this is likely too simplistic, as it could be the case that the Kuhn length is no longer the appropriate renormalization length scale: divalent ions may create a new length scale that does not appear in the monovalent solution.

In the inset to Figure 3A, the universal curves are plotted on a semilogarithmic scale. This clearly demonstrates both the logarithmic increase of length with large forces in KCl and the nonlogarithmic behavior in the divalent salts—indeed, the length is seen to depend more strongly on force for divalent salts. Caution is needed in interpreting the rescaled data, as this stronger extension variation gives the incorrect impression that the chains are longer in divalent salts than in monovalents. Instead, the correct interpretation (visible in Figure 2) is that the chains exit the 2/3 regime earlier in divalent than monovalent salt and are thus transiently shorter; the extension in divalents begins to catch up with a slightly stronger elastic response in the high-force regime. We speculate that the transiently shorter chains, and the slightly stronger elastic response, can be attributed to a slight wrapping of the polymer around condensed

divalent ions, followed by force-induced straightening of the chain. However, as we are unaware of a microscopic explanation of even the high-force logarithmic elasticity of d-ssDNA in monovalent salts, we are loathe to draw strong conclusions as to the origin of the monovalent/divalent high-force elastic difference.

CONCLUSIONS

In this paper, we report on the elasticity of denatured single-stranded DNA in various salt solutions. First, we study KCl solutions and reinforce previous conclusions found for NaCl solutions.[7,8] Within the error of the experiment we find that the two salts have nearly identical effects on d-ssDNA elasticity: at low force the data compare favorably with the "Pincus blob" theory for real polymers ($L \sim f^{2/3}$)[17] while at high force the extension varies logarithmically with force ($L \sim \ln(f)$). Quantification of the Kuhn length reveals $l \sim c^{-0.5}$, contrary to OSF theory,[9,10] while the excluded volume varies as $v \sim c^{-1}$. At high salt concentrations, the low-force nonlinear behavior is replaced by ideal elasticity, indicating a Θ point at 3−3.5 M; fits to the ideal WLC model return a persistence length for d-ssDNA of $l_p \approx 0.65$ nm.

Upon changing from monovalent ions to divalent ions, the elastic response of d-ssDNA is qualitatively similar, with a low-force Pincus regime still visible. However, the high-force elastic response, while weak, is not logarithmic, contrasting with the monovalent results. Likely the most salient results of this study involve the heightened response of d-ssDNA elasticity to changes in divalent salt concentration. This is seen in two ways:

1. The ratio between concentrations of 1:1 salt and 2:1 salt that give roughly equivalent elastic behavior is large. While naive application of mean-field theories predicts that a 3-fold ratio would result in equivalent electrostatic conditions, we measure a much larger ratio of 50−200. This ratio persists in both good solvent and Θ conditions. We quantitatively account for the ratio at the Θ point by calculating the condition for equivalent effective polymer charge density within a condensed-ion model based on strong-coupling theories. This approach predicts an increase in the ratio as salt concentration decreases from Θ; this is clearly observed for moderate concentrations of Mg, but not lower concentrations, reflecting the model's validity in only the high-salt regime. Qualitatively, the same model can explain the difference in Θ conditions for different divalent counterions (Ca^{2+} vs Mg^{2+}) based on differences in the size of the hydrated ion.
2. At low and moderate concentrations of divalent salts, we are able to collapse the force−extension data by scaling out a characteristic force $\bar{f}$ that is a function of the concentration of divalent salt. Indeed, $\bar{f}$ varied strongly with ionic strength: $\bar{f} \sim I^3$. This directly contrasts with the $I^{1/2}$ dependence of the rescaling force found in monovalent salt and could indicate an anomalously strong increase in flexibility of d-ssDNA with divalent salt concentration.

AUTHOR INFORMATION

Corresponding Author

*E-mail: saleh@engineering.ucsb.edu.

ACKNOWLEDGMENT

We thank P. Pincus for helpful conversations and the Aspen Center for Physics for its hospitality and work environment. This work was supported by the National Science Foundation under Grant DMR-1006737, by the MRSEC Program under Award DMR05-20415, and by a UCSB Materials Research Laboratory CSP Technologies fellowship to D.M.

REFERENCES

(1) Messina, R. *J. Phys.: Condens. Matter* **2009**, *21*, 18.
(2) Grosberg, A. Y.; Nguyen, T. T.; Shklovskii, B. I. *Rev. Mod. Phys.* **2002**, *74*, 329–345.
(3) Bloomfield, V. A. *Biopolymers* **1997**, *44*, 269–282.
(4) Draper, D. E. *Biophys. J.* **2008**, *95*, 5489–5495 and references therein.
(5) Liedl, T.; Hogberg, B.; Tytell, J.; Ingber, D. E.; Shih, W. M. *Nature Nanotechnol.* **2010**, *5*, 520–524.
(6) Dietz, H.; Douglas, S. M.; Shih, W. M. *Science* **2009**, *325*, 725–730.
(7) Saleh, O. A.; McIntosh, D. B.; Pincus, P.; Ribeck, N. *Phys. Rev. Lett.* **2009**, *102*, 068301–4.
(8) McIntosh, D. B.; Ribeck, N.; Saleh, O. A. *Phys. Rev. E* **2009**, *80*, 7.
(9) Odijk, T. *J. Polym. Sci., Part B: Polym. Phys.* **1977**, *15*, 477–483.
(10) Skolnick, J.; Fixman, M. *Macromolecules* **1977**, *10*, 944–948.
(11) McMaster, G. K.; Carmichael, G. G. *Proc. Natl. Acad. Sci. U.S.A* **1977**, *74*, 4835–4838.
(12) Dessinges, M. N.; Maier, B.; Zhang, Y.; Peliti, M.; Bensimon, D.; Croquette, V. *Phys. Rev. Lett.* **2002**, *89*, 248102.
(13) Kasai, H.; Iwamoto-Tanaka, N.; Fukada, S. *Carcinogenesis* **1998**, *19*, 1459–1465.
(14) Ribeck, N.; Saleh, O. A. *Rev. Sci. Instrum.* **2008**, *79*, 094301–6 and references therein.
(15) Bouchiat, C.; Wang, M. D.; Allemand, J. F.; Strick, T.; Block, S. M.; Croquette, V. *Biophys. J.* **1999**, *76*, 409–413.
(16) Marko, J. F.; Siggia, E. D. *Macromolecules* **1995**, *28*, 8759–8770.
(17) Pincus, P. *Macromolecules* **1976**, *9*, 386–388.
(18) Rief, M.; Clausen-Schaumann, H.; Gaub, H. E. *Nat. Struct. Biol.* **1999**, *6*, 346–349.
(19) Dobrynin, A. V.; Carrillo, J. Y.; Rubinstein, M. *Macromolecules* **2010**, *43*, 9181–9190.
(20) Heilman-Miller, S. L.; Thirumalai, D.; Woodson, S. A. *J. Mol. Biol.* **2001**, *306*, 1157–1166.
(21) Livadaru, L.; Netz, R. R.; Kreuzer, H. J. *Macromolecules* **2003**, *36*, 3732–3744.
(22) Toan, N. M.; Thirumalai, D. *Macromolecules* **2010**, *43*, 4394–4400.
(23) Shklovskii, B. I. *Phys. Rev. E* **1999**, *60*, 5802–5811.
(24) Luan, B.; Aksimentiev, A. *J. Am. Chem. Soc.* **2008**, *130*, 15754–15755.
(25) Qiu, X. Y.; Kwok, L. W.; Park, H. Y.; Lamb, J. S.; Andresen, K.; Pollack, L. *Phys. Rev. Lett.* **2006**, 96.
(26) Qiu, X. Y.; Andresen, K.; Kwok, L. W.; Lamb, J. S.; Park, H. Y.; Pollack, L. *Phys. Rev. Lett.* **2007**, 99.